Anisotropic spin susceptibility of spin-density-wave states

X. M. Chen and A. W. Overhauser
Department of Physics, Purdue University, West Lafayette, Indiana 47907
(Received 21 May 1990; revised manuscript received 9 July 1990)

The spin response of a spin-density-wave (SDW) state arises from two contributions: a Pauli term (described by spin splitting of the Fermi surface) and an interband term resulting from virtual spin-flip transitions across the SDW energy gap. Both terms are anisotropic, and so is their sum. For a linear SDW the axis of anisotropy is the SDW polarization vector; for a spiral SDW the anisotropy axis is perpendicular to the plane of polarization. In either case the algebraic sign of the anisotropy depends on whether $Q/2k_f$ is greater than or less than unity, where Q is the SDW wave vector. The magnitude of the anisotropy (which is enhanced by exchange and correlation) can be as large as $\sim 50\%$. The hcp metals Ti, Zr, and Hf exhibit considerable anisotropy, but magnetic structure has not yet been discovered for them.

I. INTRODUCTION

The spin dependence of exchange potentials between electrons has a great influence on the ground state of an interacting electron system. For an electron gas with Coulomb interactions, it has been shown[1] that, in the Hartree-Fock approximation, the paramagnetic plane-wave state is always unstable towards the formation of a spin-density-wave (SDW) state (in which the spin density of the electrons is sinusoidally modulated). One may expect that the spin susceptibility of such a state is different from that of a free-electron gas. It is the purpose of this paper to discuss the anisotropy of the spin susceptibility of either a linear or a spiral SDW state. The study was prompted by our attempt to explain the observed anisotropy in the magnetic susceptibility of group-IV hcp metals[2] (Ti, Zr, and Hf). In Zr, for example, the magnetic susceptibility parallel to the c axis is 1.65 times larger than the perpendicular one. An explanation for this anisotropy has not yet appeared in the literature.

The model we employ here is similar to the nearly free-electron model[3] except that the SDW introduces a spin-dependent, self-consistent single-particle potential (as a result of the exchange interaction between electrons). Unlike the diamagnetic susceptibility of a charge-density-wave (CDW) state,[4] where the axis of anisotropy is the CDW $\mathbf{Q}$ vector, the anisotropy axis of the spin susceptibility in an SDW state is determined by the spin-polarization direction.

There are two terms which contribute to the spin susceptibility of a SDW. The first term is like the Pauli susceptibility which arises from the expansion or shrinkage of the Fermi surface for opposite spins. (This term is the only one for a free-electron gas.) The second term arises from the virtual spin-flip transitions between the two subbands created by the SDW energy gaps. For a linear SDW both terms contribute if the magnetic field $\mathbf{H}$ is perpendicular to the spin polarization $\hat{\mathbf{s}}$. Only the Pauli-like term enters when $\mathbf{H}$ is parallel to $\hat{\mathbf{s}}$. Electrons near the SDW energy gaps align either parallel or antiparallel to the SDW polarization direction. Consequently, these electrons contribute little to the Pauli susceptibility term when a magnetic field is applied perpendicular to $\hat{\mathbf{s}}$. Thus, the Pauli susceptibility for $\mathbf{H}$ perpendicular to $\hat{\mathbf{s}}$ is smaller than the susceptibility parallel to $\hat{\mathbf{s}}$. A detailed analysis shows that this reduction is almost cancelled by the presence of the virtual transition term. Accordingly, the anisotropy of the spin susceptibility is smaller than what one would first expect.

With the experimental data for Cr in view, some theoretical work on the spin susceptibility of a linear SDW was carried out by Fedders and Martin.[5] Using a two-band model (and assuming a perfect nesting of electron and hole sheets of the Fermi surface), they found that, at $T=0$, while the perpendicular susceptibility remains finite, the parallel one goes to zero. This conclusion will not apply to our model. Our results indicate that the perpendicular spin susceptibility can be either larger or smaller than the parallel one, depending on how the energy-gap planes passing through $\mathbf{k}=\pm\mathbf{Q}/2$ intersect the Fermi surface.

Because of the weak dependence of spin susceptibility on temperature, all calculations in this paper are made at $T=0$. We will first use the standard perturbation theory to study the spin susceptibility of a linear SDW in Sec. II, which is followed by a similar discussion in Sec. III for a spiral SDW. In Sec. IV a mixed SDW-CDW state and the influence of many-body effects are examined. We find that, for a mixed SDW-CDW state, only the SDW component causes an anisotropy in spin susceptibility and, furthermore, this anisotropy can be significantly enhanced by many-body effects. Finally, we present a summary of the evidence that Zr has a SDW.

II. SPIN SUSCEPTIBILITY OF A LINEAR SDW

A linear SDW in an electron gas occurs if the single-particle self-consistent potential is given by

$$V(\mathbf{r})=-G\sigma_x\cos\mathbf{Q}\cdot\mathbf{r}\ , \tag{1}$$

where σ_x is the usual Pauli matrix. For simplicity we assume the polarization of the SDW is along the x axis. G

is the SDW energy gap which, in general, depends on temperature. The temperature dependence of G is similar to that of the energy gap in a superconductor.[1] Since we are primarily interested in the susceptibility at low temperature, G will be taken to be a constant.

The Fermi surface of an electron gas subject to the potential (1) is shown in Fig. 1 by the solid curves. Electrons with spin $S_x=\frac{1}{2}$ and $-\frac{1}{2}$ have the same energy but, of course, their spatial wave functions differ. This degeneracy will be broken when one introduces an external magnetic field along the x axis. The Fermi surfaces then split as illustrated by the dashed curves in the same figure. The spin susceptibility (parallel to the polarization), can be found easily by just counting the number of electrons between the two Fermi surfaces, and is given by

$$\chi_{\parallel}=\mu_B^2 N(E_F)\ , \tag{2}$$

where μ_B is the Bohr magneton and $N(E_F)$ is the electron density of states at the Fermi energy E_F. If we write $\chi_{\parallel}$ in terms of the quantities χ_p and $N_0(E_F)$ for the corresponding free-electron gas, we have

$$\chi_{\parallel}=\chi_p\frac{N(E_F)}{N_0(E_F)}\ . \tag{3}$$

$N(E_F)/N_0(E_F)$ has been studied by Overhauser in Ref. 3. Figure 2 shows the behavior of $\chi_{\parallel}/\chi_p$ versus $Q/2k_F$ for several values of g_0, where $g_0\equiv G/4E_F$, and k_F is the Fermi radius of the electron gas in the absence of a SDW. Point A in Fig. 2 (for $g_0=0.05$) corresponds to the Fermi surface which makes critical contact with the energy gaps introduced by the potential (1). Point B is where electrons just begin to fill the higher-energy band. Between A and B, $\chi_{\parallel}/\chi_p$ is a straight line. At point A,

$$\begin{aligned}\chi_{\parallel}&=\chi_p(1+2g_0)^{1/2}\\ &\cong\chi_p(1+g_0)\end{aligned} \tag{4}$$

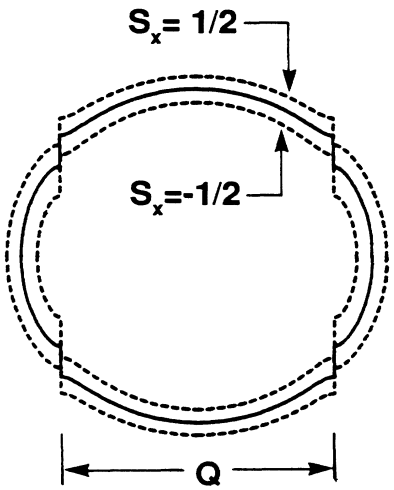

FIG. 1. Fermi surfaces of an electron gas with a linear SDW. Solid lines ——, no external magnetic field is applied. Dashed lines — — —, an external magnetic field (in the $-\hat{\mathbf{x}}$ direction) is applied along the polarization axis of the SDW.

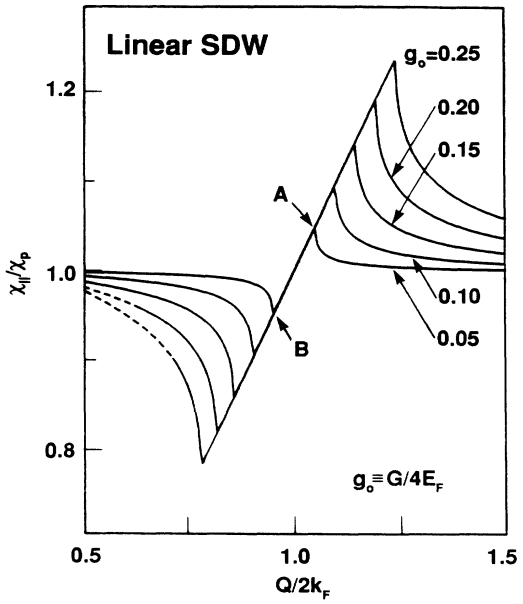

FIG. 2. Parallel spin susceptibility of a linear SDW. Dashed curves indicate regions where the calculations are less accurate.

for small g_0.

As can be seen from the above discussion, the only contribution to $\chi_{\parallel}$ comes from the splitting of the Fermi surfaces for the two different spin states, i.e., from the ordinary Pauli mechanism. This result does not apply to $\chi_{\perp}$ when the external magnetic field is perpendicular to the polarization direction of the SDW. To see how another term enters $\chi_{\perp}$, consider the Hamiltonian

$$\hat{H}=\frac{p^2}{2m}-G\sigma_x\cos\mathbf{Q}\cdot\mathbf{r}+\hat{H}' \tag{5}$$

with

$$\hat{H}'=-\mu_B H_{\text{ext}}\sigma_z\ . \tag{6}$$

H_{ext} is the magnitude of the applied external field. It is straightforward (but tedious) to show that, for $H_{\text{ext}}=0$, the eigenfunctions of $\hat{H}$ in the σ_z representation are given approximately by

$$\begin{aligned}\psi_{\mathbf{k}\uparrow}&=\frac{1}{n_{\mathbf{k}}}(u_{\mathbf{k}}e^{i\mathbf{k}\cdot\mathbf{r}}\alpha\mp v_{\mathbf{k}}e^{i(\mathbf{k}-\mathbf{Q})\cdot\mathbf{r}}\beta\\ &\qquad+w_{\mathbf{k}}e^{i(\mathbf{k}+\mathbf{Q})\cdot\mathbf{r}}\beta)\ ,\\ \psi_{\mathbf{k}\downarrow}&=\frac{1}{n_{\mathbf{k}}}(u_{\mathbf{k}}e^{i\mathbf{k}\cdot\mathbf{r}}\beta\mp v_{\mathbf{k}}e^{i(\mathbf{k}-\mathbf{Q})\cdot\mathbf{r}}\alpha\\ &\qquad+w_{\mathbf{k}}e^{i(\mathbf{k}+\mathbf{Q})\cdot\mathbf{r}}\alpha)\ ,\end{aligned} \tag{7}$$

with the energy

$$\begin{aligned}E(\mathbf{k})&=\tfrac{1}{2}(\epsilon_{\mathbf{k}}+\epsilon_{\mathbf{k}-\mathbf{Q}})\mp\tfrac{1}{2}[(\epsilon_{\mathbf{k}}-\epsilon_{\mathbf{k}-\mathbf{Q}})^2+G^2]^{1/2}\\ &\quad+\frac{G^2}{4(\epsilon_{\mathbf{k}}-\epsilon_{\mathbf{k}+\mathbf{Q}})}\ ,\end{aligned} \tag{8}$$

where $\epsilon_{\mathbf{k}}=\hbar^2k^2/2m$. α and β are the usual Pauli spinors with $S_z=\frac{1}{2}$ and $-\frac{1}{2}$. If we let $k_Q\equiv\mathbf{k}\cdot\mathbf{Q}/Q$, $-$ and $+$ in

Eq. (8) correspond, respectively, to $Q/2 > k_Q > 0$ (states below the energy gap) and $k_Q > Q/2$ (states above the energy gap).

The coefficients in Eqs. (7) are

$$u_{\mathbf{k}} = \cos\xi_{\mathbf{k}} ,$$
$$v_{\mathbf{k}} = \sin\xi_{\mathbf{k}} , \tag{9}$$
$$w_{\mathbf{k}} = \frac{G}{2(\epsilon_{\mathbf{k}+\mathbf{Q}} - \epsilon_{\mathbf{k}})} ,$$

and

$$n_{\mathbf{k}} = (1 + w_{\mathbf{k}}^2)^{1/2} ,$$

where $\cos\xi_{\mathbf{k}}$ and $\sin\xi_{\mathbf{k}}$ are determined by

$$\sin 2\xi_{\mathbf{k}} = \frac{G}{W_{\mathbf{k}}} \tag{10}$$

with $W_{\mathbf{k}} = [(\epsilon_{\mathbf{k}} - \epsilon_{\mathbf{k}-\mathbf{Q}})^2 + G^2]^{1/2}$. If one replaces $\mathbf{Q}$ by $-\mathbf{Q}$ in Eqs. (7) and (8), one finds the eigenstates and energies for $-Q/2 < k_Q < 0$, and for $k_Q < -Q/2$.

From Eq. (6), with $H_{\text{ext}} \neq 0$, the only nonzero matrix elements of $\hat{H}'$ which involve the "mostly spin-up" state $\psi_{\mathbf{k}\uparrow}$ are $\langle \psi_{\mathbf{k}\uparrow} | \hat{H}' | \psi_{\mathbf{k}\uparrow} \rangle$, $\langle \psi_{(\mathbf{k}-\mathbf{Q})\downarrow} | \hat{H}' | \psi_{\mathbf{k}\uparrow} \rangle$, and $\langle \psi_{(\mathbf{k}+\mathbf{Q})\downarrow} | \hat{H}' | \psi_{\mathbf{k}\uparrow} \rangle$. The first one provides a correction to the energy, and the other two provide corrections to the wave function of the state. The band structure and the spin-flip interband transitions are shown in Fig. 3. Up to first order in H_{ext}, the perturbed wave functions are, for "mostly spin-up" states,

$$\psi^p_{\mathbf{k}\uparrow} = \psi_{\mathbf{k}\uparrow} + \frac{\langle \psi_{(\mathbf{k}-\mathbf{Q})\downarrow} | \hat{H}' | \psi_{\mathbf{k}\uparrow} \rangle}{E_{\mathbf{k}} - E_{\mathbf{k}-\mathbf{Q}}} \psi_{(\mathbf{k}-\mathbf{Q})\downarrow} + \frac{\langle \psi_{(\mathbf{k}+\mathbf{Q})\downarrow} | \hat{H}' | \psi_{\mathbf{k}\uparrow} \rangle}{E_{\mathbf{k}} - E_{\mathbf{k}+\mathbf{Q}}} \psi_{(\mathbf{k}+\mathbf{Q})\downarrow} . \tag{11}$$

The energy correction is

$$\Delta E_{\mathbf{k}\uparrow} = -\mu_B H_{\text{ext}} \frac{(\cos 2\xi_{\mathbf{k}} - w_{\mathbf{k}}^2)}{n_{\mathbf{k}}^2} . \tag{12}$$

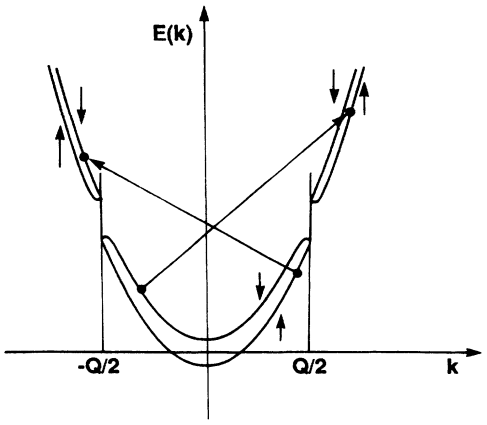

FIG. 3. The energy band structure of a linear SDW when a magnetic field is perpendicular to the polarization. Interband transitions which are highly anisotropic also contribute to the spin susceptibility.

For the "mostly spin-down" states,

$$\psi^p_{\mathbf{k}\downarrow} = \psi_{\mathbf{k}\downarrow} + \frac{\langle \psi_{(\mathbf{k}-\mathbf{Q})\uparrow} | \hat{H}' | \psi_{\mathbf{k}\downarrow} \rangle}{E_{\mathbf{k}} - E_{\mathbf{k}-\mathbf{Q}}} \psi_{(\mathbf{k}-\mathbf{Q})\uparrow} + \frac{\langle \psi_{(\mathbf{k}+\mathbf{Q})\uparrow} | \hat{H}' | \psi_{\mathbf{k}\downarrow} \rangle}{E_{\mathbf{k}} - E_{\mathbf{k}+\mathbf{Q}}} \psi_{(\mathbf{k}+\mathbf{Q})\uparrow} , \tag{13}$$

and the energy correction is

$$\Delta E_{\mathbf{k}\downarrow} = \mu_B H_{\text{ext}} \frac{(\cos 2\xi_{\mathbf{k}} - w_{\mathbf{k}}^2)}{n_{\mathbf{k}}^2} . \tag{14}$$

The $\mathbf{k}$ dependence of $\Delta E_{\mathbf{k}\uparrow}$ and $\Delta E_{\mathbf{k}\downarrow}$ in Eqs. (12) and (14) indicates that the splitting of the Fermi surfaces is no longer uniform. Indeed, as shown in Fig. 4, the external field has little effect on the electrons near the SDW energy gaps. The spin-related magnetic moment of the perturbed state $\psi^p_{\mathbf{k}\uparrow}$ is given by

$$M_{\mathbf{k}\uparrow} = \mu_B \left[\langle \psi_{\mathbf{k}\uparrow} | \sigma_z | \psi_{\mathbf{k}\uparrow} \rangle + 2\mu_B H_{\text{ext}} \frac{|\langle \psi_{(\mathbf{k}-\mathbf{Q})\uparrow} | \sigma_z | \psi_{\mathbf{k}\downarrow} \rangle|^2}{E_{\mathbf{k}-\mathbf{Q}} - E_{\mathbf{k}}} [1 - f(E_{\mathbf{k}-\mathbf{Q}})] + 2\mu_B H_{\text{ext}} \frac{|\langle \psi_{(\mathbf{k}+\mathbf{Q})\downarrow} | \sigma_z | \psi_{\mathbf{k}\uparrow} \rangle|^2}{E_{\mathbf{k}+\mathbf{Q}} - E_{\mathbf{k}}} [1 - f(E_{\mathbf{k}+\mathbf{Q}})] \right] , \tag{15}$$

where $f(E)$ is the usual Fermi-Dirac distribution function. The factors $[1 - f(E_{\mathbf{k}-\mathbf{Q}})]$ and $[1 - f(E_{\mathbf{k}+\mathbf{Q}})]$ enter because virtual transitions are allowed only from occupied states to unoccupied states. The magnetic moment $M_{\mathbf{k}\downarrow}$ of state $\psi^p_{\mathbf{k}\downarrow}$ can be obtained by interchange of $\uparrow$ and $\downarrow$ in Eq. (15). Summing $M_{\mathbf{k}\uparrow}$ and $M_{\mathbf{k}\downarrow}$ over all occupied states gives the total spin magnetic moment

$$M = \frac{1}{(2\pi)^3} \int [M_{\mathbf{k}\uparrow} f(E_{\mathbf{k}} + \Delta E_{\mathbf{k}\uparrow}) + M_{\mathbf{k}\downarrow} f(E_{\mathbf{k}} + \Delta E_{\mathbf{k}\downarrow})] d\mathbf{k}$$
$$\cong \frac{1}{(2\pi)^3} \int \left[(M_{\mathbf{k}\uparrow} + M_{\mathbf{k}\downarrow}) f(E_{\mathbf{k}}) + (M_{\mathbf{k}\uparrow} - M_{\mathbf{k}\downarrow}) \left(\frac{\partial f}{\partial E_{\mathbf{k}}} \right) \Delta E_{\mathbf{k}\uparrow} \right] d\mathbf{k} . \tag{16}$$

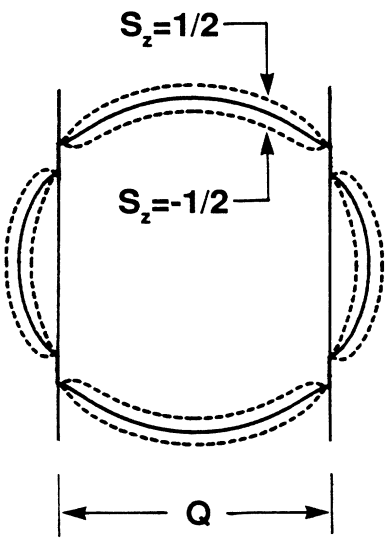

FIG. 4. Fermi surfaces of an electron gas with a linear SDW when the external magnetic field is perpendicular to the polarization axis of the SDW, and in the $-\hat{\mathbf{z}}$ direction.

At zero temperature $f(E)$ becomes the step function $\Theta(E_F-E)$ and $\partial f/\partial E \rightarrow -\delta(E-E_F)$. Substituting $M_{\mathbf{k}\uparrow}$ and $M_{\mathbf{k}\downarrow}$ into Eq. (16) and dividing by H_{ext}, we get the perpendicular spin susceptibility

$$\chi_\perp=\frac{2\mu_B^2}{(2\pi)^3}\int\left[4\frac{|\langle\psi_{(\mathbf{k}-\mathbf{Q})\downarrow}|\sigma_z|\psi_{\mathbf{k}\uparrow}\rangle|^2}{E_{\mathbf{k}-\mathbf{Q}}-E_{\mathbf{k}}}\times[1-f(E_{\mathbf{k}-\mathbf{Q}})]f(E_{\mathbf{k}})+|\langle\psi_{\mathbf{k}\uparrow}|\sigma_z|\psi_{\mathbf{k}\uparrow}\rangle|^2\left[-\frac{\partial f}{\partial E_{\mathbf{k}}}\right]\right]d\mathbf{k}\ . \quad (17)$$

The second term in Eq. (17) is just the Pauli susceptibility term arising from the splitting of the Fermi surfaces in Fig. 4. This term is smaller than the value of $\chi_\parallel$ (corresponding to the splitting shown in Fig. 1) because there are fewer states between the surfaces. This reduction, however, as we will show below, is largely compensated by the first term in Eq. (17), which arises from the virtual transitions across the SDW energy gap. In order to illustrate this result, we substitute Eqs. (7) and (8) into Eq. (17), and neglect the corrections from $w_{\mathbf{k}}$ and $G^2/4(\epsilon_{\mathbf{k}}-\epsilon_{\mathbf{k}+\mathbf{Q}})$. We find

$$\chi_\perp=\frac{4\mu_B}{(2\pi)^3}\left[\int_{k_Q>0}2\frac{G^2}{W_{\mathbf{k}}^3}\Theta(E_F-E_{\mathbf{k}})\Theta(E_{\mathbf{k}-\mathbf{Q}}-E_F)d\mathbf{k}-\int_{k_Q>0}\frac{G^2}{W_{\mathbf{k}}^2}\delta(E_{\mathbf{k}}-E_F)d\mathbf{k}\right]+\chi_\parallel+O(g^2)\ , \quad (18)$$

where Eq. (10) has been used. $O(g^2)$ includes all higher-order terms of $g=2mG/\hbar^2Q^2$ that have been omitted.

For convenience we denote the two integrals in Eq. (18) by I_1 and I_2. The surface integral I_2 is easily performed if we make a change of variables $d\mathbf{k}\rightarrow dSdE_{\mathbf{k}}/|\nabla_{\mathbf{k}}E_{\mathbf{k}}|$, where S is a surface of constant energy. In our case this reduces to

$$d\mathbf{k}\rightarrow(2\pi m/\hbar^2)dk_Q dE_{\mathbf{k}}\ ,$$

which leads to

$$I_2=\frac{2\pi m}{\hbar^2}\left[\frac{Q}{2}\right]g^2\int_{1-x_m}^{1}\frac{dx}{x^2+g^2}\ , \quad (19)$$

where $x_m=2k_m/Q$, and k_m is the maximum value for k_Q. The volume integral I_1 is more difficult. For the case in which the SDW gap intersects the Fermi surface, the states contributing to I_1 are those shadowed in Fig. 5. Since the Fermi surface has cylindrical symmetry about k_Q, it is convenient to use a cylindrical coordinate system in which I_1 becomes

$$I_1=2(2\pi)\left[\int_0^{Q-k_m}dk_Q\int_0^{k_{\rho_1}}k_\rho dk_\rho+\int_{Q-k_m}^{Q/2}dk_Q\int_{k_{\rho_2}}^{k_{\rho_1}}k_\rho dk_\rho\right]\times\frac{G^2}{[(\hbar^2Q/2m)^2(Q-2k_Q)^2+G^2]^{3/2}}\ , \quad (20)$$

where

$$k_{\rho_1}=\left[\frac{2m}{\hbar^2}(E_F+\tfrac{1}{2}W_{\mathbf{k}})-\tfrac{1}{2}k_Q^2-\tfrac{1}{2}(k_Q-Q)^2\right]^{1/2} \quad (21)$$

and

$$k_{\rho_2}=\left[\frac{2m}{\hbar^2}(E_F-\tfrac{1}{2}W_{\mathbf{k}})-\tfrac{1}{2}k_Q^2-\tfrac{1}{2}(k_Q-Q)^2\right]^{1/2}\ . \quad (22)$$

Substituting Eqs. (21) and (22) into Eq. (20) and integrating with respect to k_ρ, we obtain

$$I_1=\frac{2\pi m}{\hbar^2}\left[\frac{Q}{2}\right]g^2\left[\int_{x_m-1}^{1}\frac{x_F^2-1-x^2}{2(x^2+g^2)^{3/2}}dx+\int_{1-x_m}^{1}\frac{dx}{x^2+g^2}\right]\ , \quad (23)$$

where again the variable k_Q has been changed to

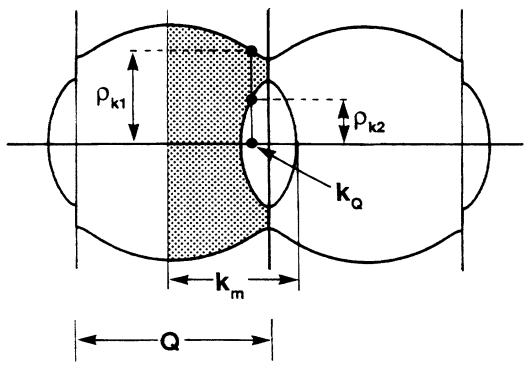

FIG. 5. Notations for the integration of Eq. (20). The range of k_Q is from 0 to k_m.

$x=2k_Q/Q$, and $x_F=2k_F/Q$. As can be seen from Eqs. (18), (19), and (23), I_2 is cancelled by the second term in I_1, and the remaining term in Eq. (18) is, in general, much smaller than I_1 or I_2 alone. It should be mentioned that this result does not depend on the magnitude of the Q vector; that is, the cancellation still occurs when $Q \geq 2k_m$. Actually, we can rewrite Eq. (18) as follows:

$$\chi_\perp = \frac{4\mu_B}{(2\pi)^3}\int_{k_Q>0}\left[\frac{G^2}{W_{\mathbf{k}}^2}\frac{\Theta(E_F-E_{\mathbf{k}})-\Theta(E_F-E_{\mathbf{k}-\mathbf{Q}})}{E_{\mathbf{k}-\mathbf{Q}}-E_{\mathbf{k}}} - \frac{G^2}{W_{\mathbf{k}}^2}\delta(E_{\mathbf{k}}-E_F)\right]d\mathbf{k}+\chi_\parallel+O(g^2)\ . \tag{24}$$

Most of the contribution to the integral comes from the small region near the energy gap at $\mathbf{k}=\mathbf{Q}/2$. However, in this region we have

$$\frac{\Theta(E_F-E_{\mathbf{k}})-\Theta(E_F-E_{\mathbf{k}-\mathbf{Q}})}{E_{\mathbf{k}-\mathbf{Q}}-E_{\mathbf{k}}}\rightarrow\delta(E_{\mathbf{k}}-E_F) \tag{25}$$

for small g. This is why I_2 is largely compensated by I_1.

For the case of critical contact, we have from Eqs. (18), (19), and (23),

$$\chi_\perp=\chi_\parallel(1-g_0)+O(g^2) =\chi_p+O(g^2)\ , \tag{26}$$

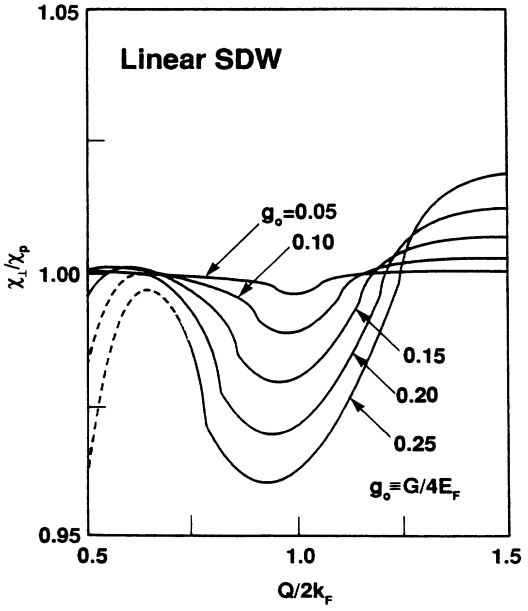

FIG. 6. Perpendicular spin susceptibility of a linear SDW. Dashed curves indicate regions where the calculations are less accurate.

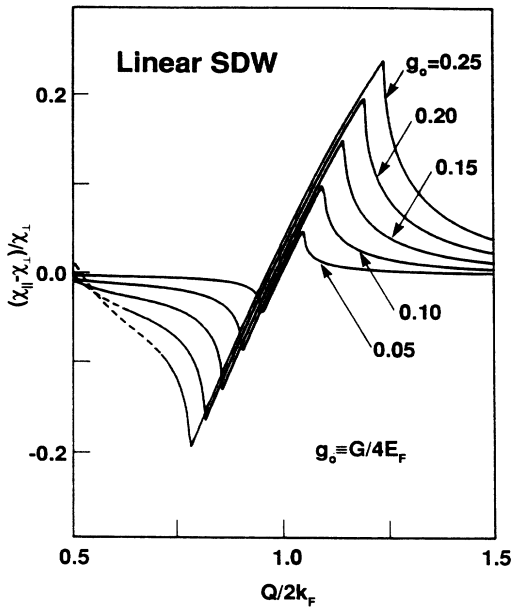

FIG. 7. Anisotropy of the spin susceptibility for a linear SDW.

where Eq. (4) has been used in the last step. To calculate $\chi_\perp$ accurately to second order in g, we have to evaluate the integrals in Eq. (17) numerically. Figure 6 shows the relation between $\chi_\perp/\chi_p$ and $Q/2k_F$ for several g_0's. Notice that $g=(2k_F/Q)^2 g_0$, and remember that the approximation for the wave functions (7) are valid only when g is much smaller than unity. Therefore, our results for small Q's are less accurate (if we keep g_0 constant), and this is indicated in Figs. 2 and 6 by the dashed lines. The anisotropy of the spin susceptibility $(\chi_\parallel-\chi_\perp)/\chi_\perp$ versus $Q/2k_F$ is plotted in Fig. 7, which clearly illustrates that the anisotropy can be either positive or negative depending on the location of the SDW energy gaps relative to the (undistorted) Fermi surface.

III. SPIN SUSCEPTIBILITY OF A SPIRAL SDW

In a spiral SDW state, an electron gas possesses a constant fractional spin polarization at every point, whereas the direction of the polarization varies in a helical fashion as a function of position. The self-consistent single-particle Hamiltonian for such a state can be written as

$$\hat{H}_0=\frac{p^2}{2m}-\frac{G}{2}(\sigma_x\cos\mathbf{Q}\cdot\mathbf{r}+\sigma_y\sin\mathbf{Q}\cdot\mathbf{r})\ , \tag{27}$$

where G is the SDW energy gap. The second term in Eq. (27), the SDW potential, connecting plane waves of wave vectors $\mathbf{k}$ and $\mathbf{k}+\mathbf{Q}$ having opposite spins, can be visualized as a superposition of two linear SDW potentials with polarizations perpendicular to each other. Eigenfunctions of $\hat{H}_0$ can be found easily by solving a 2×2 matrix equation exactly. For "mostly spin-up" states,

$$\psi_{\mathbf{k}\uparrow}=\begin{cases}\cos\xi_{\mathbf{k}\uparrow}e^{i\mathbf{k}\cdot\mathbf{r}}\alpha-\sin\xi_{\mathbf{k}\uparrow}e^{i(\mathbf{k}+\mathbf{Q})\cdot\mathbf{r}}\beta, & k_Q>-\dfrac{Q}{2}\ ,\\ \cos\xi_{\mathbf{k}\uparrow}e^{i\mathbf{k}\cdot\mathbf{r}}\alpha+\sin\xi_{\mathbf{k}\uparrow}e^{i(\mathbf{k}+\mathbf{Q})\cdot\mathbf{r}}\beta\rangle, & k_Q<-\dfrac{Q}{2}\ ,\end{cases} \tag{28}$$

with energy

$$E_{\mathbf{k}\uparrow}=\begin{cases}\frac{1}{2}(\epsilon_{\mathbf{k}}+\epsilon_{\mathbf{k}+\mathbf{Q}})-\frac{1}{2}[(\epsilon_{\mathbf{k}}-\epsilon_{\mathbf{k}+\mathbf{Q}})^2+G^2]^{1/2}, & k_Q>-\dfrac{Q}{2}\ ,\\ \frac{1}{2}(\epsilon_{\mathbf{k}}+\epsilon_{\mathbf{k}+\mathbf{Q}})+\frac{1}{2}[(\epsilon_{\mathbf{k}}-\epsilon_{\mathbf{k}+\mathbf{Q}})^2+G^2]^{1/2}, & k_Q<-\dfrac{Q}{2}\ ,\end{cases} \tag{29}$$

and for "mostly spin down" states,

$$\psi_{\mathbf{k}\downarrow}=\begin{cases}\cos\xi_{\mathbf{k}\downarrow}e^{i\mathbf{k}\cdot\mathbf{r}}\beta-\sin\xi_{\mathbf{k}\downarrow}e^{i(\mathbf{k}-\mathbf{Q})\cdot\mathbf{r}}\alpha\rangle, & k_Q<\dfrac{Q}{2}\ ,\\ \cos\xi_{\mathbf{k}\downarrow}e^{i\mathbf{k}\cdot\mathbf{r}}|\beta+\sin\xi_{\mathbf{k}\downarrow}e^{i(\mathbf{k}-\mathbf{Q})\cdot\mathbf{r}}\alpha\rangle, & k_Q>\dfrac{Q}{2}\ ,\end{cases} \tag{30}$$

with energy

$$E_{\mathbf{k}\downarrow}=\begin{cases}\frac{1}{2}(\epsilon_{\mathbf{k}}+\epsilon_{\mathbf{k}-\mathbf{Q}})-\frac{1}{2}[(\epsilon_{\mathbf{k}}-\epsilon_{\mathbf{k}-\mathbf{Q}})^2+G^2]^{1/2}, & k_Q<\dfrac{Q}{2}\ ,\\ \frac{1}{2}(\epsilon_{\mathbf{k}}+\epsilon_{\mathbf{k}-\mathbf{Q}})+\frac{1}{2}[(\epsilon_{\mathbf{k}}-\epsilon_{\mathbf{k}-\mathbf{Q}})^2+G^2]^{1/2}, & k_Q>\dfrac{Q}{2}\ ,\end{cases} \tag{31}$$

where $\xi_{\mathbf{k}\sigma}$ ($\sigma=\uparrow$ or $\downarrow$) is given by

$$\sin2\xi_{\mathbf{k}\sigma}=\frac{G}{W_{\mathbf{k}\sigma}} \tag{32}$$

and

$$W_{\mathbf{k}\sigma}=[(\epsilon_{\mathbf{k}}-\epsilon_{\mathbf{k}\pm\mathbf{Q}})^2+G^2]^{1/2}\ . \tag{33}$$

In the last formula $\sigma=\uparrow$ (or $\downarrow$) corresponds to the + (or −) sign. As implied in Eqs. (29) and (31), the SDW potential of Eq. (27) creates an energy gap at $\mathbf{k}=-\mathbf{Q}/2$ for state $\psi_{\mathbf{k}\uparrow}$, and at $\mathbf{k}=\mathbf{Q}/2$ for state $\psi_{\mathbf{k}\downarrow}$. We define $\chi_\perp$ as the susceptibility along the z axis, i.e., perpendicular to the SDW polarization plane, and $\chi_\parallel$ as the susceptibility along the x axis, which is within the polarization plane.

A. Perpendicular susceptibility $\chi_\perp$

If we regard $\hat{H}'=-\mu_B H_{\text{ext}}\sigma_z$ as a perturbation, the only nonzero matrix elements of $\hat{H}'$, involving the state $\psi_{\mathbf{k}\uparrow}$, are $\langle\psi_{\mathbf{k}\uparrow}|\hat{H}'|\psi_{\mathbf{k}\uparrow}\rangle$ and $\langle\psi_{(\mathbf{k}+\mathbf{Q})\downarrow}|\hat{H}'|\psi_{\mathbf{k}\uparrow}\rangle$. Following the procedures in Sec. II, $\chi_\perp$ is given by

$$\chi_\perp=\frac{2\mu_B}{(2\pi)^3}\int\left[\frac{2\sin^2 2\xi_{\mathbf{k}\uparrow}}{W_{\mathbf{k}\uparrow}}\Theta(E_F-E_{\mathbf{k}\uparrow})\Theta(E_{(\mathbf{k}+\mathbf{Q})\downarrow}-E_F)+\cos^2 2\xi_{\mathbf{k}\uparrow}\delta(E_{\mathbf{k}\uparrow}-E_F)\right]d\mathbf{k} \tag{34}$$

$$=\chi_p\frac{Q}{2k_F}\left[\frac{x_{m1}+x_{m2}}{2}+\frac{(x_F^2-1)}{4}\frac{x}{(x^2+g^2)^{1/2}}\Bigg|_{|x_{m1}-1|}^{x_{m2}+1}+\frac{g^2}{4}\left[\frac{x}{(x^2+g^2)^{1/2}}-\ln[x+(x^2+g^2)^{1/2}]\right]\Bigg|_{|x_{m1}-1|}^{x_{m2}+1}\right], \tag{35}$$

where $x_{m1}=2k_{m1}/Q$ and $x_{m2}=2k_{m2}/Q$. k_{m1} and k_{m2} are the maximum values of $|\mathbf{k}|$ along the $-\mathbf{Q}$ and $+\mathbf{Q}$ directions, and $\mathbf{k}$ lies on the Fermi surface of the "mostly spin-up" electrons. Plots of Eq. (35) for several values of g_0 are shown in Fig. 8. Similar to Eq. (18), Eq. (35) indicates that, to first order in g, $\chi_\perp$ is equal to χ_p at $x_{m1}\cong 1$ or $|x_{m1}-1|\gg g$.

B. Parallel susceptibility $\chi_\parallel$

In this case, the perturbation $\hat{H}'=-\mu_B H_{\text{ext}}\sigma_x$ connects $\psi_{\mathbf{k}\uparrow}$ with $\psi_{\mathbf{k}\downarrow}$, $\psi_{(\mathbf{k}-\mathbf{Q})\uparrow}$, $\psi_{(\mathbf{k}+\mathbf{Q})\uparrow}$, and $\psi_{(\mathbf{k}+2\mathbf{Q})\downarrow}$. Note that now $\langle\psi_{\mathbf{k}\uparrow}|\hat{H}'|\psi_{\mathbf{k}\uparrow}\rangle=0$ and $\langle\psi_{\mathbf{k}\uparrow}|\hat{H}'|\psi_{\mathbf{k}\downarrow}\rangle\neq 0$. Since $E_{\mathbf{k}\uparrow}\neq E_{\mathbf{k}\downarrow}$ except for $k_Q=0$, we can still use standard nondegenerate perturbation theory to calculate the susceptibility $\chi_\parallel$, which is found to be

$$\chi_{\parallel}=\frac{2\mu_B^2}{(2\pi)^3}\int\left[\frac{2\cos^2\xi_{\mathbf{k}\uparrow}\sin^2\xi_{\mathbf{k}\downarrow}}{E_{(\mathbf{k}-\mathbf{Q})\uparrow}-E_{\mathbf{k}\uparrow}}[f(E_{\mathbf{k}\uparrow})-f(E_{(\mathbf{k}-\mathbf{Q})\downarrow})]+\frac{\sin^2\xi_{(\mathbf{k}+\mathbf{Q})\uparrow}\sin^2\xi_{\mathbf{k}\uparrow}}{E_{(\mathbf{k}+2\mathbf{Q})\downarrow}-E_{\mathbf{k}\uparrow}}[f(E_{\mathbf{k}\uparrow})-f(E_{(\mathbf{k}+2\mathbf{Q})\downarrow})]\right.$$
$$\left.+\frac{\cos^2\xi_{\mathbf{k}\uparrow}\cos^2\xi_{\mathbf{k}\downarrow}}{E_{\mathbf{k}\downarrow}-E_{\mathbf{k}\uparrow}}[f(E_{\mathbf{k}\uparrow})-f(E_{\mathbf{k}\downarrow})]\right]d\mathbf{k}\ . \tag{36}$$

For small g, the second term in the integrand can be neglected because its contribution is proportional to g^3. The third term in Eq. (36) corresponds to the surface term (i.e., the Pauli term) in Eq. (17). This is understood from the following expansion for $g \ll 1$:

$$f(E_{\mathbf{k}\uparrow})-f(E_{\mathbf{k}\downarrow})=\delta(E_{\mathbf{k}\uparrow}-E_F)(E_{\mathbf{k}\downarrow}-E_{\mathbf{k}\uparrow})$$
$$+\tfrac{1}{2}\delta'(E_{\mathbf{k}\uparrow}-E_F)$$
$$\times(E_{\mathbf{k}\downarrow}-E_{\mathbf{k}\uparrow})^2+\cdots\ . \tag{37}$$

At critical contact, i.e., when $Q/2k_F\cong 1+g_0$, we find to first order in g_0

$$\chi_{\parallel}\cong\chi_p(1+\tfrac{1}{4}g_0)\ . \tag{38}$$

Therefore, for critical contact, the spin-susceptibility anisotropy of a spiral SDW state is, approximately, a quarter of that of a linear SDW having the same energy gap G. Figure 9 shows plots of $\chi_{\parallel}/\chi_p$ versus $Q/2k_F$ for several values of $g_0(=G/4E_F)$. The anisotropy of the susceptibility $(\chi_{\parallel}-\chi_{\perp})/\chi_{\perp}$ is shown in Fig. 10.

IV. DISCUSSION

A. Spin susceptibilities of a mixed SDW-CDW state

In Sec. II, we have studied the spin-susceptibility anisotropy of a linear SDW. A generalization of such a state is a mixed SDW-CDW state[3] in which both the charge density and the spin density vary sinusoidally in space. The self-consistent single-particle potential for a mixed SDW-CDW state can be written as

$$V(\mathbf{r})=-G(\sin\phi\,\sin\mathbf{Q}\cdot\mathbf{r}+\sigma_x\cos\phi\,\cos\mathbf{Q}\cdot\mathbf{r})\ , \tag{39}$$

where ϕ is the spin-split phase which can vary from 0 to $\pi/2$, corresponding to a change from a pure SDW state to a pure CDW state. The Fermi surfaces caused by the potential (39) are similar to those shown in Fig. 1. Since there is still no contribution to the parallel susceptibility $\chi_{\parallel}^{\rm mix}$ from virtual transitions, $\chi_{\parallel}^{\rm mix}$ is given again by Eqs. (2) and (3). It is conceivable that the anisotropy of the spin susceptibility may only be related to the second term in Eq. (39). Detailed derivations show that the perpendicular susceptibility can be expressed as

$$\chi_{\perp}^{\rm mix}=(\chi_{\perp}-\chi_{\parallel})\cos^2\phi+\chi_{\parallel}\ . \tag{40}$$

This result suggests that the spin-susceptibility anisotropy of a mixed SDW-CDW state is

$$\frac{\chi_{\parallel}^{\rm mix}-\chi_{\perp}^{\rm mix}}{\chi_{\perp}^{\rm mix}}=\frac{(\chi_{\parallel}-\chi_{\perp})\cos^2\phi}{\chi_{\perp}+(\chi_{\parallel}-\chi_{\perp})\sin^2\phi}\ , \tag{41}$$

where $\chi_{\parallel}$ and $\chi_{\perp}$ are the susceptibilities of a pure SDW [i.e., $\phi=0$ in Eq. (39)]. When $\phi=\pi/2$, the anisotropy goes to zero, as is expected for a nonmagnetic state.

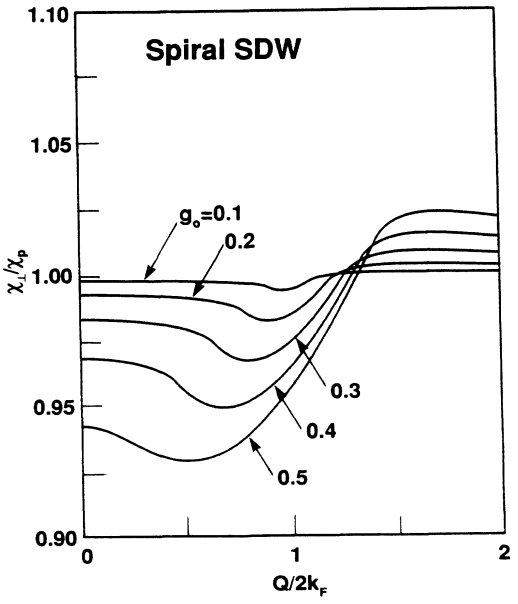

FIG. 8. Perpendicular spin susceptibility of a spiral SDW.

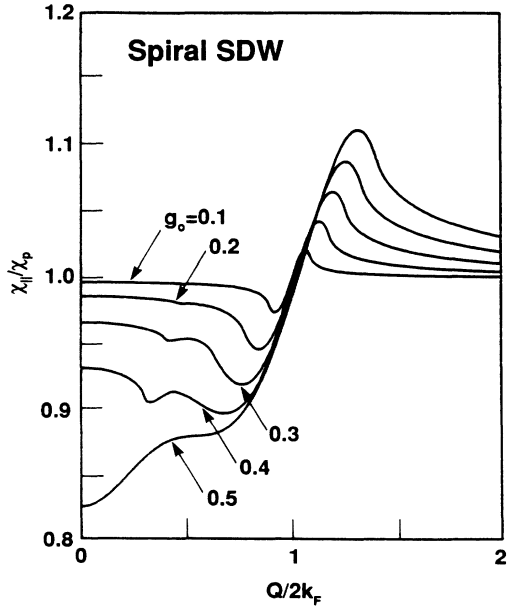

FIG. 9. Parallel spin susceptibility of a spiral SDW.

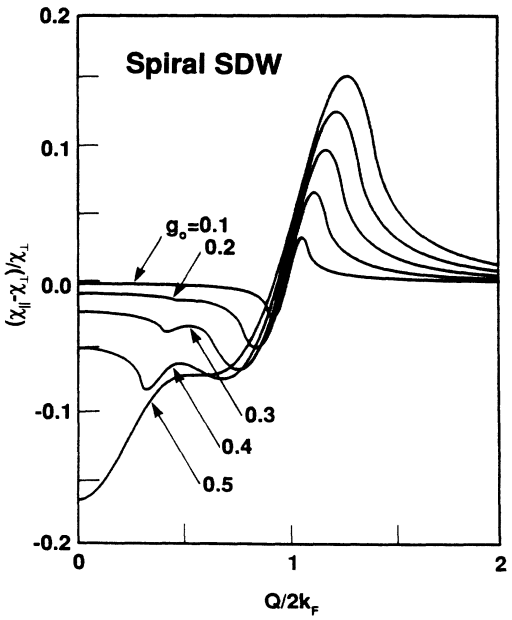

FIG. 10. Anisotropy of the spin susceptibility for a spiral SDW.

B. Influence of many-body effects

Up to now, in our discussion of χ, we have neglected the influences of exchange and correlation interactions between electrons. It is well known that one of the effects of these interactions is to enhance the spin susceptibility of an electron gas, as indicated by the well-known result

$$\chi^{\mathrm{EC}}=\frac{\chi}{1-\gamma(\chi/\chi_p)}\ , \tag{42}$$

where χ^{EC} is the spin susceptibility including many-body effects, and γ is a positive constant. At electron densities comparable to that in sodium, the increase in χ^{EC} over χ is about a factor of 2. The increase in platinum[6] is higher, probably of the order of 5. A schematic argument about Eq. (42) can be found in Ref. 7.

What we wish to emphasize here is that, according to Eq. (42), many-body effects enhance not only the magnitude of the spin susceptibility but also its anisotropy. In the case of a linear SDW, for example, take $g_0=0.15$ and let the SDW gap be in critical contact with the Fermi surface. From Sec. II we know that

$$\chi_\parallel\cong(1+g_0)\chi_p=1.15\chi_p\ ,$$

and that $\chi_\perp\cong\chi_p$. Substituting $\chi_\parallel$ or $\chi_\perp$ into Eq. (42), and for $\gamma=0.6$, we find $\chi_\parallel^{\mathrm{EC}}\cong1.50\chi_\perp^{\mathrm{EC}}$. This anisotropy is comparable to those found[2] for Ti, Zr, and Hf, as noted in the Introduction. At present there is no direct evidence for SDW's in these metals. However, there has been considerable interest in several unexplained properties of Zr which can all be understood if Zr has a longitudinally polarized SDW with $\mathbf{Q}=(2\pi/c)(001)$.

C. Evidence for a SDW in Zr

The 60% anisotropy of the magnetic susceptibility in hcp Zr would require (according to the theory presented here) a SDW polarization vector $\hat{\mathbf{s}}$ parallel to the hexagonal c axis. Zr also has an anomaly in its phonon spectrum,[8] which can be explained[9] if it has a linear SDW with $\mathbf{Q}=(2\pi/c)(001)$. A "frozen-phonon" calculation[10] has suggested that the Zr phonon anomaly might be attributed to a band degeneracy which splits during the vibration of the zone-center optical mode, but it was necessary to assume that Fermi-Dirac occupation factors followed the electronic energy shifts instantaneously (despite the fact that the optical phonon involved is the highest-frequency mode of the phonon spectrum).

The influence of SDW's on lattice dynamics has been developed previously[11] and it was suggested that the long-standing anomalies in the phonon spectrum of Pb might be caused by a family of SDW's with $\mathbf{Q}=(2\pi/a)\{210\}$. If we tentatively adopt the hypothesis that Zr has a (001) SDW with $\hat{\mathbf{s}}$ also along [001], then the SDW is longitudinally polarized. A free-electron SDW which is longitudinally polarized is invisible to magnetic neutron scattering since then $\nabla\times\mathbf{B}=0$ (and, of course, $\nabla\cdot\mathbf{B}=0$). It follows that (microscopically) $\mathbf{B}=0$ and, therefore, there would be no interaction between the SDW and a neutron's magnetic moment. The only way to find a *nearly free-electron* longitudinal SDW would be to observe magnetic satellites at $\mathbf{Q}+\mathbf{G}$, where $\mathbf{G}$ is a reciprocal-lattice vector (not parallel to $\mathbf{Q}$). Such satellites would be extremely weak because of the small admixture of $\mathbf{k}+\mathbf{G}$ wave-function components into the plane waves of wave vector $\mathbf{k}$ (caused, of course, by the weak crystal potential).

Field-induced magnetic scattering of neutrons at the reciprocal-lattice vectors $\{\mathbf{G}\}$ has been studied and was found to be isotropic.[12] The implication is that the magnetic polarization caused by conduction electrons in Zr must arise from s-wave components (which have negligible form factors at nonzero $\{\mathbf{G}\}$). The theory of the magnetic response of conduction electrons[13] which includes both orbital paramagnetism and Landau diamagnetism (in addition to Pauli paramagnetism) has been applied to the case of Zr.[14] The magnetic response was found to be essentially isotropic. Therefore, there is no "conventional" way to reconcile the observed magnetic anisotropy with either neutron scattering or standard theory. We therefore suggest the possibility (based on the present work) that Zr has a nearly free-electron SDW, polarized longitudinally, with $\mathbf{Q}=(2\pi/c)(001)$. This interpretation is consistent with the magnetic anisotropy,[2] the lack of anisotropic magnetic scattering[12] for $\mathbf{G}\neq0$, and the behavior[8] of the optical phonons near $\mathbf{q}=0$. It is also of interest to note that the proposed $\mathbf{Q}$ is nearly equal to the spanning vector of the Zr Fermi surface[15] along the [001] direction, a condition that favors the formation of a SDW ground state.[1]

ACKNOWLEDGMENTS

This research was supported by the National Science Foundation, Condensed Matter Theory Program.

[1]A. W. Overhauser, Phys. Rev. Lett. **4**, 462 (1960); Phys. Rev. **128**, 1437 (1962).
[2]E. W. Collings and J. C. Ho, Phys. Rev. B **4**, 349 (1971).
[3]A. W. Overhauser, Phys. Rev. **167**, 691 (1968); Phys. Rev. B **29**, 7023 (1984).
[4]M. L. Boriack, Phys. Rev. Lett. **44**, 208 (1980).
[5]P. A. Fedders and P. C. Martin, Phys. Rev. **143**, 245 (1965); also see, C. A. Moyer and S. Arajs, Phys. Rev. B **14**, 1233 (1976).
[6]B. Giovanni, M. Peter, and J. R. Schrieffer, Phys. Rev. Lett. **12**, 736 (1964).
[7]R. F. Watson and A. J. Freeman, Phys. Rev. **152**, 566 (1966).
[8]C. Stassis, J. Zarestky, O. D. McMasters, and B. N. Harmon, Phys. Rev. B **18**, 2632 (1978).
[9]X. M. Chen and A. W. Overhauser, Phys. Rev. B (to be published).
[10]S. H. Liu, C. Stassis, and K.-M. Ho, Phys. Rev. B **24**, 5093 (1981).
[11]X. M. Chen and A. W. Overhausser, Phys. Rev. B **39**, 10 570 (1989).
[12]C. Stassis, G. Kline, B. N. Harmon, R. M. Moon, and W. C. Koehler, J. Magn. Magn. Mater. **14**, 303 (1979).
[13]K. H. Oh, B. N. Harmon, S. Liu, and S. K. Sinha, Phys. Rev. B **14**, 1283 (1976).
[14]S. H. Liu, A. J. Liu, and J. F. Cooke, Phys. Rev. B **36**, 9521 (1987).
[15]P. M. Everett, Phys. Rev. B **6**, 3553 (1972); **20**, 1419 (1979).

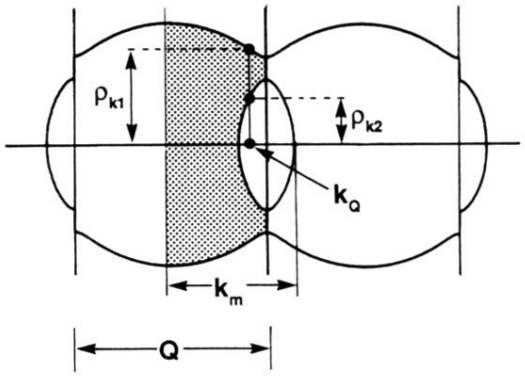

FIG. 5. Notations for the integration of Eq. (20). The range of k_Q is from 0 to k_m.